Nanosecond near-spinodal homogeneous boiling of water superheated by a pulsed CO_2 laser

Sergey I. Kudryashov,* Kevin Lyon, and Susan D. Allen
Department of Physics, Arkansas State University, State University, Arkansas 72467-0419, USA
(Received 6 May 2006; revised manuscript received 10 January 2007; published 27 March 2007)

The fast boiling dynamics of superheated surface layers of bulk water cavitating under near-spinodal conditions during nanosecond CO_2 laser heating pulses was studied using contact broad-band photoacoustic spectroscopy. Characteristic pressure-tension cycles recorded by an acoustic transducer at different incident laser fluences represent (a) weak random oscillations of transient nanometer-sized near-critical bubbles-precursors and (b) well-defined stimulated oscillations of micron-sized supercritical bubbles and their submicrosecond coalescence products. These findings provide an important insight into basic thermodynamic parameters, spatial and temporal scales of bubble nucleation during explosive liquid/vapor transformations in absorbing liquids ablated by short laser pulses in the thermal confinement regime.

DOI: 10.1103/PhysRevE.75.036313 PACS number(s): 47.55.dd, 64.70.Fx, 43.35.+d, 52.38.Mf

I. INTRODUCTION

Explosive boiling of a free superheated liquid in the thermal confinement regime is known to take place in a transition region of the thermodynamic pressure-temperature (P,T) phase diagram near the liquid-vapor spinode curve, where incoherent, spontaneous homogeneous nucleation of separate vapor bubbles merges with coherent spinodal decomposition of the corresponding superheated liquid correlated over a long scale [1,2]. Classical homogeneous nucleation theory predicts metastability of the bulk superheated liquid with respect to noninteracting finite fluctuations of its local entropy S and volume V values representing bubbles of finite critical and supercritical radii $(r \geq r_{cr})$ [1,2]. At increasing degrees of superheating, the Gibbs free energy barrier $\Delta G(T,P,r)$ for critical bubble formation and surface tension of the superheated liquid σ tend simultaneously to zero when approaching its liquid/vapor spinode curve [1], and so does r_{cr} (in practice, size-dependent $\sigma(r) \approx C_1 - C_2 r \approx C_1$ for $r \rightarrow 0$ and the numerical constants C_1 and C_2 [3], so there should be a small, but finite r_{cr} value even at the liquid/vapor spinode). At the spinode—the ultimate stability limit of the superheated liquid with regard to infinitely small thermal and/or acoustic perturbations δS, δV—a nonsteady state liquid/vapor transformation known as "spinodal decomposition" occurs, according to the Cahn-Hillard model [4], as strongly correlated large-scale fluctuations at characteristic wavelengths $\lambda \rightarrow \infty$ increasing exponentially in time (as compared to small-scale fluctuations) and setting up a large-scale spatial periodic structure, while at higher temperatures—beyond the spinode—characteristic λ continuously decreases vs increasing T to atomic or molecular dimensions in the vapor phase. However, if intense thermal fluctuations are explicitly taken into account in spinodal decomposition theory [5], the sharp spinodal curve "washes out" because the probabilities of fluctuations for *all* λ values grow towards their asymptotic equilibrium magnitudes and, thus, homogeneous nucleation and spinodal decomposition regimes merge together in the near-spinode transition region characterized by a single finite effective characteristic size of fluctuations. Despite these and other theoretical efforts [1,2,5], such combined dynamics of homogeneous nucleation and spinodal decomposition in superheated liquids near their corresponding liquid/vapor spinodes is not yet well understood.

Recently, such initial stages of fast liquid/vapor transformation have been studied in superheated liquid argon near its liquid/vapor spinode using a molecular dynamics (MD) approach [6]. In qualitative agreement with results of homogeneous nucleation theory, these studies demonstrate shorter and shorter induction (incubation) times for nucleation of nanometer-sized density fluctuations (subcritical or near-critical bubbles) in 9.5-nm MD cells vs increasing T while approaching picosecond values at temperatures $T \approx 0.9 T_{crit}$. However, since collective (correlation) and other size effects crucial for bubble nucleation in the near-spinodal region have not been included in these small-scale simulations, their important results may require experimental verification that has not been performed to date (for example, recent time-resolved x-ray scattering studies [7] of water boiling on surface of gold nanoparticles heated by femtosecond laser pulses imitate near-surface boiling of bulk superheated liquids, but not completely).

In this paper we report the use of contact broadband photoacoustic spectroscopy to study nanosecond near-spinodal homogeneous nucleation of multiple steam bubbles in a micrometer-thick layer on a free water surface superheated by a nanosecond CO_2 laser above its explosive boiling threshold. Multi-MHz oscillations of acoustic pressure recorded at different incident laser fluences have revealed a broad weak high-frequency spectral band and a number of strong highly reproducible low-frequency spectral lines interpreted, respectively, as weak random oscillations of short-living nm-sized near-critical and stimulated synchronous oscillations of μm-sized supercritical steam bubbles and their coalescence products. Important thermodynamic and kinetic parameters of near-spinodal bubble nucleation on laser-superheated surfaces of absorbing liquids in the thermal confinement regime were estimated using these experimental findings.

*Author to whom correspondence should be addressed (now with P. N. Lebedev Physical Institute, Russian Academy of Science); Electronic addresses: skudryashov@astate.edu and sergeikudryashov@yahoo.com

II. EXPERIMENTAL SETUP

In these photoacoustic experiments we used an experimental setup described elsewhere [8]. A 10.6-μm, transversely excited atmospheric (TEA) CO_2 laser beam (Lumonics 100-2, TEM_{00}, 0.1 J/pulse, the initial spike of duration $\tau_1 \approx 70$ ns [full width at half maximum (FWHM)] storing about $\gamma_1 \approx 50\%$ of the pulse energy, the pulse tail of the duration $\tau_2 \approx 0.6$ μs, repetition rate of 1 Hz) was focused by a ZnSe spherical lens (focal distance $L=10$ cm, Gaussian focal spot radius $\sigma_{1/e} \approx 0.2$ mm) at normal incidence onto a free surface of bulk high-pure de-ionized water in a cylindrical plastic container (height $H \approx 8$ mm, diameter $D \approx 14$ mm). The water obtained using a commercial deionizer was refreshed in the container after each few shots because of significant water jet expulsion occurring on a millisecond timescale. Laser energy was varied using a number of clear polyethylene sheets (20% attenuation per piece) and measured in each pulse by splitting off a part of the beam to a pyroelectric detector (Gentec ED-500) with digital readout. The front quartz window (thickness $h \approx 3$ mm) of a fast acoustic transducer ($LiNbO_3$ piezocrystal, flat response in the 1–100 MHz range) served as the bottom of the water container. A LeCroy storage oscilloscope (Wavepro 940) was used to record voltage transients [delayed by the 7–8 μs needed for the corresponding acoustic pressure transients $p(t)$ to propagate in the water volume and the quartz window] from the transducer. The relatively small laser spot on the water surface provided photoacoustic measurements in the acoustic far field resulting in differential shapes of recorded transients strongly distorted by diffraction [the diffraction parameter $(H+h)/L_D(f) \sim 1-10$, where $L_D(f)=\pi f \sigma_{1/e}{}^2/C_l \sim 1-10$ mm is the diffraction length [9] for acoustic pulses with characteristic frequencies $f=10-10^2$ MHz and the speeds of sound in water, $C_l \approx 1.4$ km/s [10]]. Moreover, according to the values of the non-linear attenuation coefficient for water, $\alpha/f^2 \approx (2.42-2.5)\times 10^{-14}$ s^2/m for $f=7-1.9\times 10^2$ MHz [10], multi-MHz components of the acoustic transients are not subject to significant attenuation when propagated in the 8-mm thick water volume. Acoustic reverberations in the water volume and acoustic delay line exhibiting periods of 10–11 and 2 μs, respectively, were not present in fast Fourier transform (FFT) spectra (Origin 7, OriginLab) of the acoustic transients taken for the first μs after the beginning of the CO_2 laser pulse to study nanosecond bubble nucleation and boiling dynamics.

III. EXPERIMENTAL RESULTS AND DISCUSSION

Photoacoustic studies performed at various incident laser fluences $F=0.8-11$ J/cm^2 show characteristic waveforms $p(t)$ consisting of a main pulse ($t=0-0.15$ μs) and an oscillatory tail at $t>0.15$ μs (Fig. 1). The main thermoacoustic pulse increases slowly for $F \leqslant F_B=1.7\pm 0.3$ J/cm^2, but then rises rapidly at fluences exceeding this well-defined explosive boiling threshold of water [8]. The sharp character of the threshold and its good agreement with previously reported magnitudes for water [11], i.e., independence on secondary

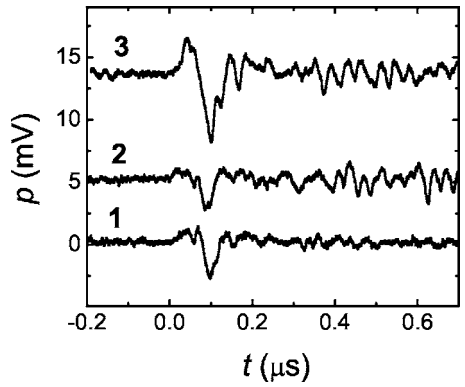

FIG. 1. Oscillatory tails ($t>0.1$ μs) of acoustic waveforms at $F \approx 0.8$ J/cm$^2 \leqslant F_1$ (1), $F_1 \leqslant 1.4 \leqslant F_2$ (2), and $2.1 \geqslant F_2$ (3) J/cm^2.

experimental conditions such as external water contamination, indicates the intrinsic bulk (homogeneous) nature of the water boiling process rather than the alternative heterogeneous boiling on surfaces of multisized contaminating particulates of different chemical composition (e.g., soot particles [11]) providing very broad (diffuse) boiling threshold (see, e.g., Ref. [7]). In support of this conclusion, near the threshold the main acoustic pulse representing the thermoacoustic response of bulk water transforms from tripolar to bipolar (see transients 1–3 in Fig. 1), where both the tripolar and bipolar waveforms are first time derivatives of the actual bipolar and unipolar waveforms generated during the laser spike (their FWHM equal that of the laser spike) via the thermoacoustic or explosive boiling mechanisms [9,12], respectively, and slightly perturbed by surface vaporization [11] and cavitation in the superheated water. The differential effect results from diffraction of the acoustic transients in the far field [9] where data acquisition was performed, and explains slower increase of the compressive pressure amplitude p_{comp} at higher $F \approx 4-5$ J/cm^2 after its initial rapid rise at $F \geqslant F_B$ [8] by large increase of the lateral size for the explosively boiling region in the superheated interfacial water layer vs F. Visible formation of a single mm-sized surface bubble and expulsion of a multi-mm water jet accompanying laser ablation for $F>F_B$ and clearly visualized in imaging studies [13] also strongly supports the explosive boiling character of the threshold F_B.

The conclusion about explosive water boiling at $F \geqslant F_B$ is also confirmed by simple energy balance analysis. Explosive boiling of water occurs during the laser pulse near its liquid/vapor spinode at positive pressures P ($P_0=1$ atm $<P<P_{cr}$) and temperatures $T \approx (0.9-1)T_{cr} \approx (5.9-6.5)\times 10^2$ K [1,10] (the critical pressure and temperature of water are $P_{cr} \approx 22.4$ MPa and $T_{cr} \approx 647$ K [10], respectively) in the "thermal confinement" regime [6], when the threshold volume energy density $\varepsilon_{th} \approx (1-R)F_{th}/\delta \approx 1\times 10^3$ J/cm^3 [1] is supplied by the incident laser fluence $F_{th} \approx 0.9$ J/cm^2 for $R \leqslant 0.01$ [14] and $\delta \approx 9$ μm [15] (the reflectivity and penetration depth for a flat surface of bulk water at normal incidence and 10.6-μm laser wavelength, respectively). For increasing total laser fluence F, the onset of laser-induced explosive boiling in water at the instantaneous fluence $F(t) \approx F_{th}$ can be achieved at an earlier time instant t during the

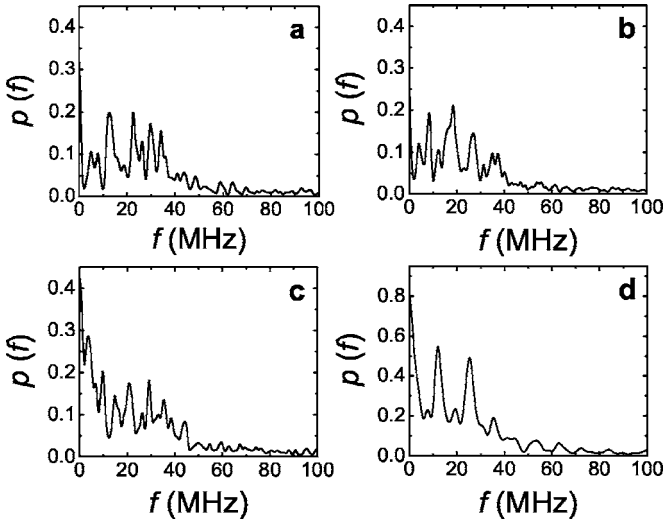

FIG. 2. Amplitude FFT spectra for the time interval $t=0.2-0.9$ μs of acoustic waveforms at different $F(\mathrm{J/cm^2})$: (a) 1.4, (b) 1.7, (c) 3.5, and (d) 6.5.

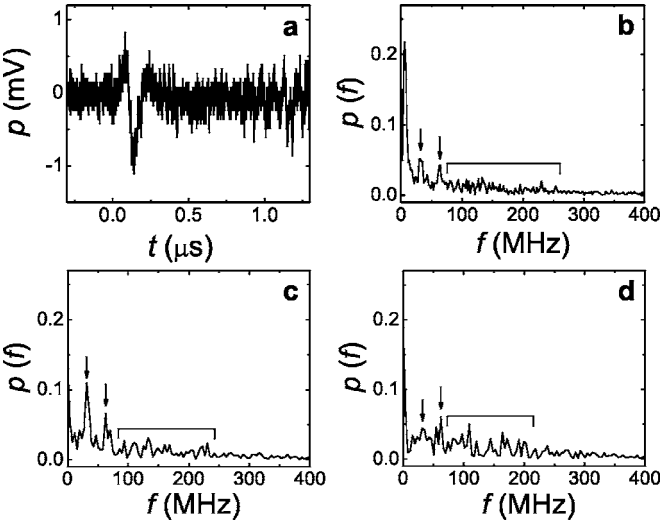

FIG. 3. Acoustic waveform at $F\approx 2.1$ J/cm^2 (a) and amplitude FFT spectra of its slices over the intervals $t=0-0.3$ μs (b), 0.3–0.5 μs (c), and 0.5–0.7 μs (d) showing transient abundances of different steam bubbles. The arrows show positions of 32- and 63-MHz modes and the horizontal bracket shows position of the diffuse band (see the text for details).

CO_2-laser heating pulse and can be resolved in time using the nanosecond acoustic transducer. For example, for the 50:50 energy content ratio of the CO_2-laser spike and tail there are two reference total fluence thresholds $F_1\approx 0.9$ J/cm^2 and $F_2\approx 1.8$ J/cm^2 ($F_2\approx F_1/\gamma_1\approx 2F_1$), which should provide explosive boiling of water at the end of the tail ($t\approx 0.75$ μs) and spike ($t=0.15$ μs), respectively. Therefore, at $F_1\leqslant F\leqslant F_2$ one can see the bipolar main thermoacoustic pulse accompanied by oscillatory boiling (cavitation) signal during the laser pulse tail, while at $F\geqslant F_2$ the explosive boiling effect and, to a minor extent, surface vaporization builds up the main unipolar explosive expansion pulse and the accompanying cavitation signal [11]. Note that, according to the energy balance analysis and experimental data of other studies, surface vaporization of water starts at lower $F\approx 0.3$ J/cm^2 [11], corresponding to the normal boiling temperature $T_{\mathrm{boil}}\approx 373$ K at $P=P_0$ [10].

In accordance with the reference thresholds F_1 and F_2, at $F\approx 0.8$ J/cm$^2\leqslant F_1$ only the symmetric tripolar main thermoacoustic pulse was recorded followed for $t>0.2$ μs by a few low-amplitude oscillations at a background level (transient 1 in Fig. 1). In contrast, at $F\approx 1.4$ J/cm^2 $>F_1$ the asymmetric tripolar main pulse is accompanied for $t>0.4$ μs (after the laser spike) by a pronounced oscillatory tail (transient 2 in Fig. 1) representing characteristic fast (nanosecond) cavitation dynamics of steam bubbles with resonant frequencies $f\approx 10-40$ MHz [Fig. 2(b)], which μs-scale dynamics has been studied in our previous work [16]. The amplitude FFT spectra in Fig. 2 were obtained for the first 0.7-μs ($t=0.2-0.9$ μs) slices of this and other acoustic transients for $F>F_1$. The well-resolved characteristic spectral peaks of various bubbles in Fig. 2 confirm their formation via homogeneous nucleation in superheated water, rather than via heterogeneous boiling on surfaces of a multitude of contaminating particulates responding acoustically in a broadband frequency range. Importantly, it is homogeneous boiling that provides in bulk liquids high volume density of similar nucleation centers for sufficient energy dissipation near corresponding liquid/vapor spinode curves, comparing to heterogeneous bubble nucleation on contaminating particulates or air/gas bubbles [1]. At higher $F\approx 2.1$ J/cm$^2\geqslant F_2$ an oscillatory tail starts at the end of the laser spike at $t\geqslant 0.1$ μs (transient 3 in Fig. 1). Surprisingly, the spectral amplitudes of bubble modes in Fig. 2 do not change significantly for $F<6$ J/cm^2 in spite of increasing axial and radial dimensions of the superheated surface water layer, while in agreement with the abovementioned F-independent onset of explosive boiling at $F(t)\approx F_{\mathrm{th}}$ and the virtual diffraction-limited increase of p_{comp} at $F=1.7-6$ J/cm^2 at the slowly increasing actual p_{comp} amplitude [8]. Altogether these facts demonstrate that under our experimental conditions the explosive boiling process is driven by thermodynamic (e.g., degree of superheating) rather than kinetic (e.g., heating rate) factors and exhibits a *single* threshold F_{th} for different total (integral over the laser pulse) laser fluences $F>F_{\mathrm{th}}$, indicating explosive boiling at some fixed superheating limit which could be the liquid/vapor spinode (see below). Also, the main oscillation modes in Fig. 2 show their damping during the laser tail with characteristic times of about 1 μs consistent with our previous measurements [16].

More complex, but noisy acoustic transients exhibiting higher-resolution FFT spectra more rich in higher f were obtained at $F\approx 2.1$ J/cm^2 (Fig. 3) using thinner water layers ($H\approx 1-1.5$ mm), since, in this case, the diffraction effect for the multi-MHz acoustic waves is considerably weaker. In particular, the bubble oscillation mode at $f\approx 32$ MHz in Fig. 3 has much shorter lifetime (≈ 150 ns according to its FWHM parameter $\Gamma\approx 6$ MHz) than the other modes in Fig. 2, while another mode at $f\approx 63$ MHz exhibits slightly longer lifetime ≈ 250 ns ($\Gamma\approx 4$ MHz in Fig. 3). Potentially, the latter mode could be the second harmonic of the former one with its lifetime longer because of higher thermal agita-

tion, similarly to the most spectral peaks in Fig. 2. Supercritical steam bubbles representing both of these modes may be the precursors of the larger bubbles coalesced on a nanosecond time scale [17] from the smaller ones and oscillating at lower $f<30$ MHz as shown in Figs. 2 and 3.

Furthermore, FFT spectra in Fig. 3 show also a weak diffuse band at $f\approx 70-250$ MHz with the central frequency $f_C\approx 1.6\times 10^2$ MHz and FWHM parameter $\Gamma\approx 1\times 10^2$ MHz, which has the average amplitude at the level of rf noise from the CO_2-laser gas discharge. We believe that this band may represent a multitude of transient near-critical steam bubbles (rather than nonoscillating periodic spinodal structures) which are smaller, rapidly oscillating precursors of the larger, slowly oscillating 32- and 63-MHz supercritical bubbles and grow very slowly and randomly for $(dr/dt)=0$ and $(d^2r/dt^2)=0$ at $r=r_{cr}$ [18] driven presumably by a random force $\Psi(T,P,r,t)$ resulting from thermal fluctuations. Indeed, the Gibbs free energy $\Delta G(T,P,r)$ for homogeneous nucleation of bubbles has a maximum at $r\approx r_{cr}$ and the thermodynamic driving force for bubble growth $\Phi(T,P,r,t)=(\partial\Delta G/\partial r)_{T,P},r_{cr}\approx 0$, defining the critical bubble radius as $r_{cr}=2\sigma(P,T)/[P_S(T)-P_0]$ [1,2] where $P_S(T)$ is the saturated vapor pressure at T. For $\Phi(T,P,r,t)$ negligible near $r\approx r_{cr}$ such critical and near-critical bubbles have a chance to make a few random oscillations forth and back (random acts of growth and shrinkage) under the influence of $\Psi(T,P,r,t)$ during their slow evolution in size and frequency domains in the near-critical region, emitting a number of short and low-amplitude acoustic wave packets with random frequencies and phases at strongly broadened linewidths, as seen in Fig. 3 from the close correspondence of the f_C and Γ magnitudes of bubble oscillations in the band. The number of near-critical bubbles per unit volume and periods of their near-critical oscillations are strong (exponential) functions of T [1,2]. Therefore, one can expect to observe such random oscillations of tiny near-critical bubbles in FFT spectra in the form of a very weak and broad band with amplitudes and central frequencies rapidly changing versus F, which seems to be the case in this work.

Since critical bubbles are "bottleneck species" in the homogeneous nucleation kinetics exhibiting the minimal possible growth rates [1,2,18], their oscillation frequencies $f\sim f_C$ characterize a bubble nucleation frequency $f_{nucl}(P,T,r_{cr})$, the parameter used to define at a given P,T a steady-state homogeneous nucleation rate $J(P,T)=N_0(P,T)B\exp[-\Delta G(P,T,r_{cr})/kT]$, where $N_0(P,T)\sim 10^{22}$ cm^{-3} is the density of molecules in a liquid and $B\sim 10^{10-12}$ Hz is the kinetic prefactor [1,2]. The product $B\exp[-\Delta G(P,T,r_{cr})/kT]=f_{nucl}(P,T,r_{cr})$ and, as a result, for explosive boiling conditions assumed in this work— $T^*\approx 0.9T_{cr}\approx 5.9\times 10^2$ K, $P_S(T^*)\approx 8.6\times 10^6$ Pa [10] and $f_{nucl}[P_S(T^*),T^*,r_{cr}]\approx f_C\approx 1.6\times 10^2$ MHz—one finds $\Delta G[P_S(T^*),T^*,r_{cr}]\approx(4-8)\times 10^{-20}$ J. Simultaneously, one can write for $\Delta G(P,T,r_{cr})=\frac{1}{3}(4\pi r_{cr}^2)\sigma(P,T)=(2/3)\pi r_{cr}^3[P_S(T)-P_0]$ [1], which gives for the known $\Delta G[P_S(T^*),T^*,r_{cr}]$ and $[P_S(T^*)-P_0]$ the estimate $r_{cr}\approx 1.5-2$ nm consistent with $r_{cr}\sim 1-3$ nm in Refs. [2,6]. Moreover, for the known r_{cr} and $\Delta G[P_S(T^*),T^*,r_{cr}]$ one can estimate $\sigma[P_S(T^*),T^*]=3\Delta G[P_S(T^*),T^*,r_{cr}]/(4\pi r_{cr}^2)\approx(4-5)\times 10^{-3}$ N/m, which corresponds, according to data for $\sigma(P_S,T_S)$ on the water binode curve [10], to the near-spinodal explosive boiling temperature $T^*\approx 6.2\times 10^2$ K $\approx 0.95T_{cr}$ in good agreement with the energy balance analysis above and typical spinodal temperatures $T_{spin}(P>0)>0.92T_{cr}$ for real liquids [1].

When these critical steam bubbles grow to supercritical dimensions blown up by $P_S(0.95T_{cr})$, their maximum diameter D_{max} for maximal $f\approx 32$ MHz can approach $D_{max}(32\text{ MHz})\approx 6\ \mu\text{m}\leqslant\delta\approx 9\ \mu$m [14] calculated using the Rayleigh's formula [17] written as $D_{max}\approx 1.1[P_S(0.9T_{cr})/\rho(0.9T_{cr}))^{1/2}/f$ and values of the water density $\rho(6.2\times 10^2\text{ K})\approx 0.5\times 10^3$ kg/m^3 [1] and $P_S(6.2\times 10^2\text{ K})\approx 1.5\times 10^7$ Pa [10]. This result shows single-layer packaging of the supercritical bubbles in the superheated interfacial water layers of the thickness $\leqslant\delta$ supporting bubble growth as compared to the underlying mm-thick cooler water layers. Also, it explains why acoustic waves nearly coherently emitted by the bubbles of similar sizes can be readily recorded in the normal direction in the acoustic far field without significant attenuation by other bubbles or loss of coherence of their oscillations in the recorded signals. As a result, the subsequent nanosecond coalescence of these micron-sized bubbles presumably occurs within the micron-thick superheated water layers along their surface.

IV. CONCLUSIONS

In this work we have demonstrated that transient micron-sized supercritical steam bubbles grow and coalesce on a nanosecond timescale in a thin surface layer of free bulk water superheated by the TEA CO_2 laser. We have also revealed some indications of random oscillations of nanometer-sized near-critical steam bubbles nucleating and growing toward supercritical sizes, and estimated their dimensions, nucleation frequency, and work of formation, as well as temperature and surface tension of the superheated water at the explosive boiling threshold. The extracted bubble nucleation parameters and energy balance analysis indicate explosive boiling of the superheated water near its liquid/vapor spinode curve. These results provide new insight into near-spinodal explosive boiling of laser-superheated liquids in the thermal confinement regime.

ACKNOWLEDGMENTS

The authors are grateful to National Science Foundation (Grant No. 0218024) and A.A. Karabutov for financial and technical support, respectively.

[1] V. P. Skripov, E. N. Sinitsyn, P. A. Pavlov, G. V. Ermakov, G. N. Muratov, N. V. Bulanov, and V. G. Baidakov, *Thermophysical Properties of Liquids in the Metastable State* (Gordon and Breach, New York, 1988).
[2] P. G. Debenedetti, *Metastable Liquids: Concepts and Principles* (Princeton University Press, Princeton, 1996).
[3] R. C. Tolman, J. Chem. Phys. **17**, 333 (1949).
[4] J. W. Cahn and J. E. Hillard, J. Chem. Phys. **31**, 688 (1959).
[5] H. E. Cook, Acta Metall. **18**, 297 (1970); J. S. Langer, Ann. Phys. (N.Y.) **65**, 53 (1971).
[6] E. Leveugle, D. S. Ivanov, and L. V. Zhigilei, Appl. Phys. A **79**, 1643 (2004).
[7] V. Kotaidis, C. Dahmen, G. von Plessen, F. Springer, and A. Plech, J. Chem. Phys. **124**, 184702 (2006), and references therein.
[8] S. I. Kudryashov, K. Lyon, and S. D. Allen, Proc. SPIE **6086**, 60861Y (2006).
[9] V. E. Gusev and A. A. Karabutov, *Laser Optoacoustics* (AIP, New York, 1993).
[10] I. S. Grigor'ev and E. Z. Meilikhova, *Fizicheskie Velichini* (Energoatomizdat, Moscow, 1991).
[11] F. V. Bunkin, A. A. Kolomensky, V. G. Mikhailevich, S. M. Nikiforov, and A. M. Rodin, Sov. Phys. Acoust. **32**, 21 (1986); A. F. Vitshas, L. M. Dorozhkin, V. S. Doroshenko, V. V. Korneev, L. P. Menakhin, and A. P. Terentiev, *ibid.* **34**, 43 (1988).
[12] S. I. Kudryashov, Ph.D. thesis, Moscow State University, 1999.
[13] G. Paltauf and H. Schmidt-Kloiber, Appl. Phys. A **62**, 303 (1995); K. Hatanaka, M. Kawao, Y. Tsuboi, H. Fukumura, and H. Masuhara, J. Appl. Phys. **82**, 5799 (1997); D. Kim and C. P. Grigoropoulos, Appl. Surf. Sci. **127-129**, 53 (1998); I. Apitz and A. Vogel, Proc. SPIE **4961**, 48 (2003).
[14] *Handbook of Optical Constants of Solids*, edited by E. D. Palik (Academic Press, Orlando, 1991).
[15] R. K. Shori, A. A. Walston, O. M. Stafsudd, D. Fried, and J. T. Walsh, Jr., IEEE J. Sel. Top. Quantum Electron. **7**, 959 (2001).
[16] S. I. Kudryashov, K. Lyon, and S. D. Allen, Phys. Rev. E **73**, 055301(R) (2006).
[17] K. F. MacDonald, V. A. Fedotov, S. Pochon, B. F. Soares, N. I. Zheludev, C. Guignard, A. Mihaescu, and P. Besnard, Phys. Rev. E **68**, 027301 (2003).
[18] S. van Stralen and R. Cole, *Boiling Phenomena: Physicochemical and Engineering Fundamentals and Applications* (Hemisphere Publishing Corp., Washington, 1979).